Conformational studies of chiral D-Lys-PNA and achiral PNA system in binding with DNA or RNA through a molecular dynamics approach

ARTICLE *in* EUROPEAN JOURNAL OF MEDICINAL CHEMISTRY · AUGUST 2014

Impact Factor: 3.45 · DOI: 10.1016/j.ejmech.2014.08.015 · Source: PubMed

3 AUTHORS, INCLUDING:

Ida Autiero
Italian National Research Council
9 PUBLICATIONS **86** CITATIONS
SEE PROFILE

Michele Saviano
Italian National Research Council
247 PUBLICATIONS **2,937** CITATIONS
SEE PROFILE

European Journal of Medicinal Chemistry xxx (2014) 1–9

Contents lists available at ScienceDirect

European Journal of Medicinal Chemistry

journal homepage: http://www.elsevier.com/locate/ejmech

Original article

Conformational studies of chiral D-Lys-PNA and achiral PNA system in binding with DNA or RNA through a molecular dynamics approach

Ida Autiero [a], Michele Saviano [b, *], Emma Langella [a, **]

[a] National Research Council, Institute of Biostructures and Bioimaging, 80134 Naples, Italy
[b] National Research Council, Institute of Crystallography, 70126 Bari, Italy

ARTICLE INFO

Article history:
Received 22 May 2014
Received in revised form
31 July 2014
Accepted 1 August 2014
Available online xxx

Keywords:
Peptide nucleic acid
RNA
Molecular dynamics
DNA
Conformation

ABSTRACT

The growing interest in peptide nucleic acid (PNA) oligomers has led to the development of a very wide variety of PNA derivatives. Among others, the introduction of charged chiral groups on a PNA oligomer has proven effective in improving DNA binding ability, complexation direction and cellular uptake. In particular, the introduction of three adjacent chiral monomers based on D-Lys in the middle of the PNA sequence (D-Lys-PNA) has produced noteworthy results in modulating the directionality of the binding with the DNA complementary strand and in mismatch detection. Here, through a molecular dynamics approach, a comparative study has been carried out to investigate the structural properties that drive the interaction of the chiral D-Lys-PNA and the corresponding achiral PNA system with DNA as well as RNA complementary strands, starting from the crystal structure of D-Lys-PNA in complex with DNA. The results obtained complement experimental data and indicate that the binding with the RNA molecule, compared to DNA, is differently affected by the addition of three D-Lys groups on the PNA backbone, suggesting that this modification could be taken into account for the development of new PNA-based molecules able to discriminate between DNA and RNA.

1. Introduction

A peptide nucleic acid (PNA) is a DNA mimic molecule with an N-(2-aminoethyl) glycine peptidic backbone in place of the usual sugar phosphodiester one. PNA is able to bind complementary DNA and RNA sequences via Watson–Crick hydrogen bonding (WC-hb) to form hybrid duplexes more stable than the corresponding DNA–DNA or RNA–RNA duplexes [1,2]. The very high PNA binding-specificity to the complementary oligomer sequence and its resistance against natural enzymes are remarkable advantages and render this system promising for biomedical research [3]. Currently, PNA finds useful applications in various areas of diagnostics and therapeutics: this system is used for gene induction, for inhibition of translation, and also as probe to identify specific gene sequences or to recognize even a single gene mutation [4–9].

A large number of interesting PNA derivatives have been proposed to improve binding properties, overcoming PNA limitations such as solubility, cellular delivery and DNA/RNA discrimination [10–19]. Indeed, incorporating charged and chiral groups on the PNA backbone has proven effective in improving DNA binding ability, complexation direction and cellular uptake [20]. In particular, the introduction of three adjacent chiral monomers based on D-Lys (called “chiral box”) in the middle of the PNA sequence (D-Lys-PNA) has been demonstrated to be very useful for modulating the directionality of the binding with the DNA complementary strand, binding selectivity and mismatch detection [21–23]. The resulting D-Lys-PNA–DNA (LPD) duplex has also been characterized from a structural point of view by means of X-ray crystallography, providing insights into the overall duplex structure [24].

However, to date, very few structures of PNA–DNA and PNA–RNA heteroduplexes have been solved [24–28], particularly for modified PNA, although the effect of PNA modifications on the duplex conformational preferences, as well as on the binding discrimination between DNA and RNA, is of particular interest. In line with the increasing interest toward this research area, various computational studies have been reported in the last years on PNA and modified PNA [19,29–38] in order to gain insights into their conformational features (structure, flexibility, etc…) and recognition capabilities. Indeed, structural studies play a key role for the design and the improvement of PNA molecules to be used as antisense reagents or diagnostic probes.

* Corresponding author.
** Corresponding author.
E-mail addresses: msaviano@unina.it (M. Saviano), emma.langella@cnr.it (E. Langella).

http://dx.doi.org/10.1016/j.ejmech.2014.08.015
0223-5234/

In this context, we have employed molecular dynamics (MD) simulations to perform a comparative structural study on the chiral D-Lys-PNA and the corresponding achiral PNA in complex with the fully complementary strand of DNA (LPD and PD systems) as well as RNA (LPR and PR systems) (Fig. 1), starting from the crystallographic structure of LDP, which has been used as a template to create the duplex systems under investigation. As PNAs are non standard residues for force fields currently used in MD packages, we have used our own PNA force field parameters. The latter parameters have been derived and implemented in the GROMACS package, and their validity has been checked in our previous work [39].

The results obtained from the comparison between the different heteroduplexes are able to give an atomic-level description of the effect of PNA chirality, due to the introduction of three lysine groups in the middle of a PNA sequence, on the binding with DNA and RNA, thus complementing experimental data.

2. Method

The crystallographic structure of the LPD duplex was downloaded from the Protein Data Bank database (PDB id: 1NR8) [24] and modified by removing terminal capping groups, ions and water molecules from the coordinate file. Then, only the DNA and PNA coordinates were considered and used as templates to create the models of the PD, LPR and PR duplex systems. In detail, PD was created by removing the D-lysine side chain from the PNA backbone of the three central residues (in positions 5, 6 and 7), the LPR duplex was created by replacing the deoxy-ribose with the ribose sugar moiety in the DNA strand and the nucleobases of thymine residues with those of uracil, (adding the OH functional group in position 2′ of the sugar moiety of the DNA strand) in each residue. Finally the PR system was created by removing all the D-lysine side-chains held by the PNA strand from the previously obtained LPR system. All the systems have been minimized and subjected to molecular dynamics (MD) simulations.

MD simulations were performed and analyzed using the GROMACS simulation package [40]. The Parmbsc0 [41] force field, a refinement of the AMBER parm99 [42] force field for nucleic acids, was employed for the simulations. Since the PNA residues are not recognized by the force field, these parameters were manually assigned according to the procedure described in our previous work [39].

Subsequently, the models were solvated in an octahedral box filled with TIP3P water molecules with at least 9 Å distance to the border adding counter-ions to neutralize the system. The simulations were run under NPT conditions (300 K and $P = 1$ bar) with the Berendsen coupling algorithm [43]. Periodic boundary conditions were employed and the LINCS algorithm [44] was used to constrain all bond lengths. The particle mesh Ewald method was applied to treat electrostatic interactions [45,46], and a non bonded cutoff of 1.4 nm was used for the Lennard-Jones potential. In all the systems, the water molecules were relaxed by energy minimization and followed by 10 ps of simulations at 300 K, restraining the PNA and DNA/RNA atomic positions with a harmonic potential. Then, all the systems were heated up gradually to 300 K in a five step process, starting from 50 K. After this step, the systems were simulated in NPT standard conditions for 300 ns without restraints. The analysis of the MD trajectories was done with the GROMACS package. Free energy calculations were done by MMPBSA (molecular mechanics (MM) Poisson Boltzmann/Generalized Born surface area MM-GBSA) analysis using the MMPBSA.py program of the AmberTool suite [47,48].

3. Results

The analysis of the MD trajectories suggests that all the studied hybrid duplex structures are right stable, during the whole simulation time, except LPR. The root mean square deviation (RMSD) was calculated on each single strand composing the systems taking into account all the atoms excluding those of the terminal residues and is displayed in Fig. 2. It reveals that LPD, PD and PR systems reach equilibrium, after a few nanoseconds of simulation. On the contrary, the LPR duplex reaches equilibration slightly later and with significantly higher RMSD values, especially for the PNA strand.

The root mean square fluctuation residue profiles (Fig. 3) indicate comparable flexibility for both the hybrid strands in all the systems. The only exception is represented by the chiral PNA residues (in position 5,6,7) of LPR, which show significantly higher RMSF values.

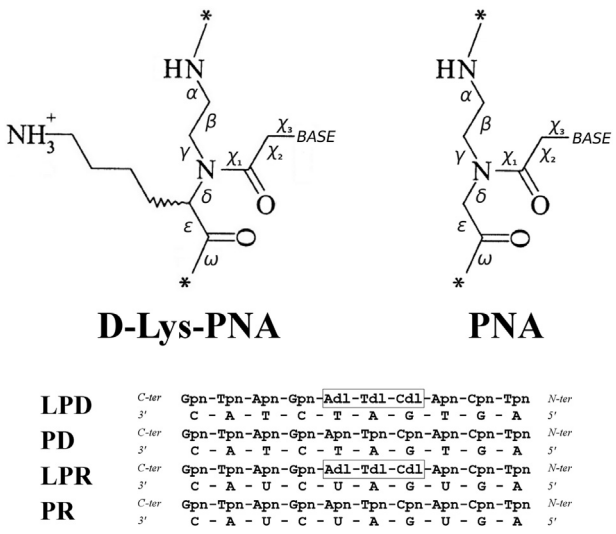

Fig. 1. Top: Chemical structure of D-Lys-PNA (left) and PNA (right) oligomers. Bottom: Sequences of the four systems studied (LPD, PD, LPR, PR). The three PNA chiral monomers ("chiral box") are boxed.

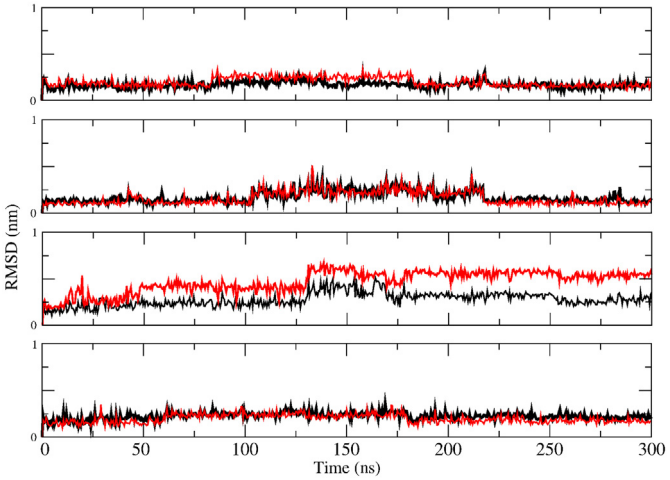

Fig. 2. From the top: Root Mean Square Deviation (RMSD) of: LPD, PD, LPR and PR systems, respectively. RMSD profiles are reported in black for the DNA and RNA strands and in red for PNA and D-Lys-PNA strands. The RMSD gives a measure of the deviation of the system (heteroduplex) from the starting conformation, as a function of the time. (For interpretation of the references to color in this figure legend, the reader is referred to the web version of this article.)

Please cite this article in press as: I. Autiero, et al., Conformational studies of chiral D-Lys-PNA and achiral PNA system in binding with DNA or RNA through a molecular dynamics approach, European Journal of Medicinal Chemistry (2014), http://dx.doi.org/10.1016/j.ejmech.2014.08.015

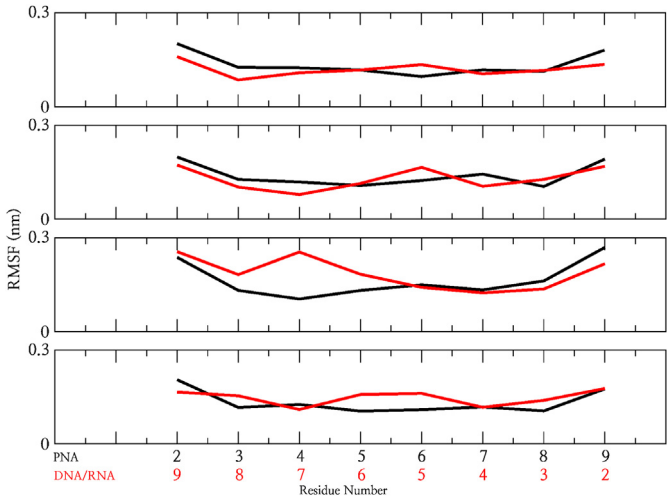

Fig. 3. From the top: Root Mean Square Fluctuation (RMSF), calculated for each residue excluding the terminals, of: LPD, PD, LPR and PR systems, respectively. RMSF profiles are reported in black for the DNA and RNA strands and in red for PNA and D-Lys-PNA strands. The RMSF gives a time-averaged measure of the deviation between the position of atom i and its starting position. (For interpretation of the references to color in this figure legend, the reader is referred to the web version of this article.)

Inter-strand Watson–Crick hydrogen bonds (WC-hbs) strongly stabilize all the duplexes. Even a temporary loss of few WC-hbs slightly affects the global stability of the system, reflecting in a small alteration of the RMSD profile. As an example, in the PD system, the small gap of the RMSD profile between 100 ns and 220 ns seems to be attributable to the temporary loss of the T6-Ad15 WC-hb (where T6 and Ad15 stand for the Thymine in position 6 of the DNA strand and the Adenine in position 5 of the PNA strand, respectively) and, similarly, in the PR system, the loss of the U3-Apn8 WC-hb, during 60- to 180-ns, hits the RMSD profile in the corresponding time range of the simulation. Notably, both the WC-hbs are rapidly regained by the systems.

Table 1
Percentage of existence of each WC-hb between the strands composing each system. From the left: LPD, PD, LPR and PR, respectively. The couple of residues involved into each WChb has been indicated using the corresponding residues positions (indicated as residue number in the Table) along the sequence.

LPD			PD			LPR			PR		
	DNA	L-PNA		DNA	PNA		RNA	L-PNA		RNA	PNA
%	Residue number		%	Residue number		%	Residue number		%	Residue number	
91	2	9	90	2	9	78	2	9	87	4	7
87	4	7	85	7	4	76	4	7	83	2	9
85	7	4	83	4	7	71	8	3	74	5	6
82	7	4	82	9	2	70	7	4	73	7	4
79	5	6	81	4	7	68	4	7	70	8	3
79	9	2	79	7	4	64	9	2	69	4	7
78	8	3	78	8	3	61	2	9	66	9	2
77	4	7	70	5	6	56	2	9	61	2	9
69	3	8	68	3	8	44	3	8	59	8	3
64	6	5	67	7	4	44	9	2	55	6	5
61	6	5	64	5	6	40	8	3	54	2	9
60	4	7	58	9	2	34	7	4	54	4	7
59	9	2	57	2	9	21	7	4	47	5	6
58	7	4	57	8	3	19	6	5	45	9	2
51	5	6	51	3	8	19	6	5	40	3	8
49	8	3	49	6	5	12	5	6	35	6	5
48	2	9	45	2	9	6	5	6	30	3	8
46	3	8	29	6	5						
33	2	9									

In Table 1 we report the percentage of existence of each WC-hb during the simulations. The percentage of existence indicates the percentage of time that a given hydrogen bond existed during the trajectory. Almost all of the allowed WC-hbs remain stable between the two strands of the LPD, PD and PR systems, as indicated by the high (50–90%) percentages of existence reported in Table 1 for these systems. In particular, for the PNA residues in positions 5, 6 and 7 (chiral box region), the percentage of WC-hbs existence is significantly higher in LPD than in PD (Fig. 4). Moreover, in this region, the LPD system maintains all the WC-hbs allowed for more than 50% of the simulation time, whilst, in the PD duplex, one WC-hb, that between residue 7 of PNA and 4 of DNA, is quickly lost. The higher percentage of occurrence of WC-hbs is suggestive of a "constrained orientation" for inter-strand base pairing in the "chiral box" region of the LPD duplex, likely due to the steric hindrance of the lysine side-chains. Instead, in the LPR system, some of the WC-hbs became less significant during the simulation, particularly in the central region of the dimer. Above all, the residues in positions 5 and 6 of PNA preserve the typical WC-hbs for less than the 20% of the total simulation time. In addition, various short-lived hydrogen bonds are detected between the PNA and RNA nucleobases either between the NH_3-Lys and the 2′-hydroxyl group of residues 5 and 6 of PNA and 4 and 5 of RNA, respectively. The propensity of the PNA-charged lysine group to interact with the 2′-hydroxyl of RNA-ribose likely interferes with the maintenance of the WC-hbs between the PNA and RNA strands and disturbs the global asset of the helix in that region.

In order to gain insights into the orientation of the lysine side-chains, we have computed, along the trajectories, the percentage of time during which the NH_3^+ groups point toward the bulk solvent, the major groove or the minor groove in both the LPD and LPR systems (see Fig. 5 caption for calculation details).

These data are represented in Fig. 5 and clearly show that the % of time spent into the bulk solvent is preponderant (c.a. 70%) for all the three positions (5,6,7) in LPD. These findings are in line with the visual inspection of the trajectory which indicates that Lys side-chains are well solvent-exposed and don't make stable interactions with either the PNA or the DNA strands.

On the other hand, there is a different situation in LPR in position 6 and, to a lesser extent, in position 5, where it emerges that the NH_3^+ groups spend a more significant percentage of time into the major and minor grooves, respectively. These findings are in agreement with data above reported, concerning hydrogen bonds detected between the NH_3-Lys and the 2′-hydroxyl group of residues 5 and 6 of PNA and 4 and 5 of RNA.

The torsional angles of the PNA strand were monitored during the entire course of the simulations (Figs. 6 and 7). No significant distortion emerges from our results, and the angle variability seems to be similar for LPD, PD and PR systems, as shown in Figs. 6 and 7. On the contrary, significant PNA dihedral distortions are present in the case of the LPR system, in particular for the β, γ and χ^2 angles (Fig. 7).

As a consequence, the overall helical structure of the duplexes is well maintained by all the systems except LPR, as shown in Fig. 8. In addition, LPR was confirmed as the less favored duplex also from an energetics point of view, showing the highest value of the free energy estimated using the MMPBSA calculation (LPR = −41.3 kcal/mol, LPD = −51.7 kcal/mol, PD = −51.9 kcal/mol and PR = −53.2 kcal/mol).

4. Discussion and conclusion

Employing the published LPD heteroduplex crystal structure [24], we have created a model of a PNA–DNA heterodimer complex without chiral groups on the PNA backbone (PD), and the

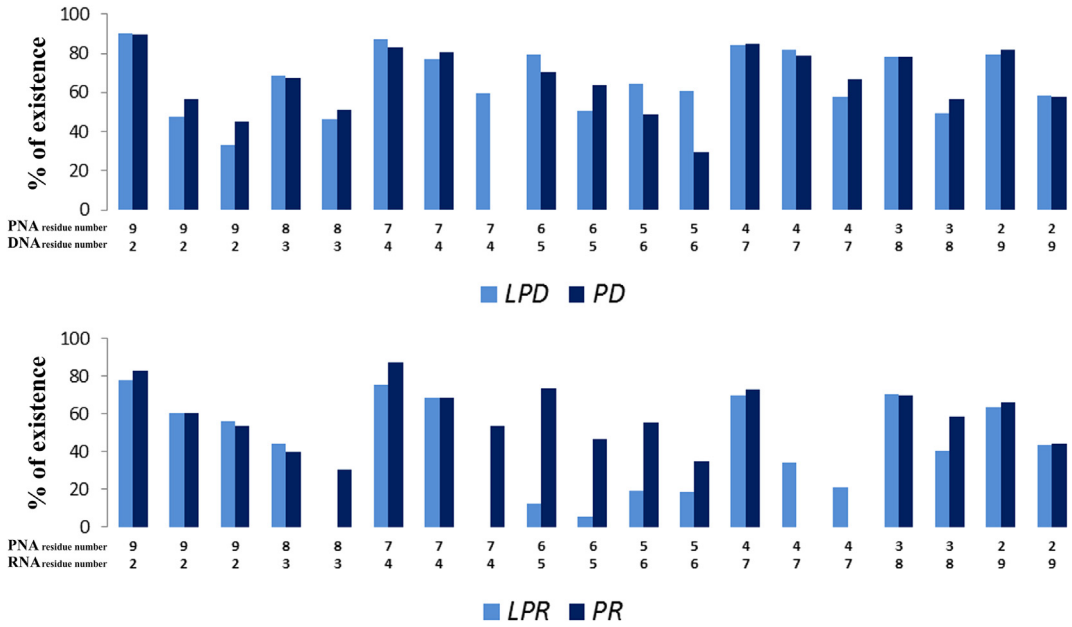

Fig. 4. Percentage of existence of each WC-hb between the strands composing each system, shown in histogram form. Top: LPD and PD systems in light and dark blue, respectively. Bottom: LPR and PR systems in light and dark blue, respectively. (For interpretation of the references to color in this figure legend, the reader is referred to the web version of this article.)

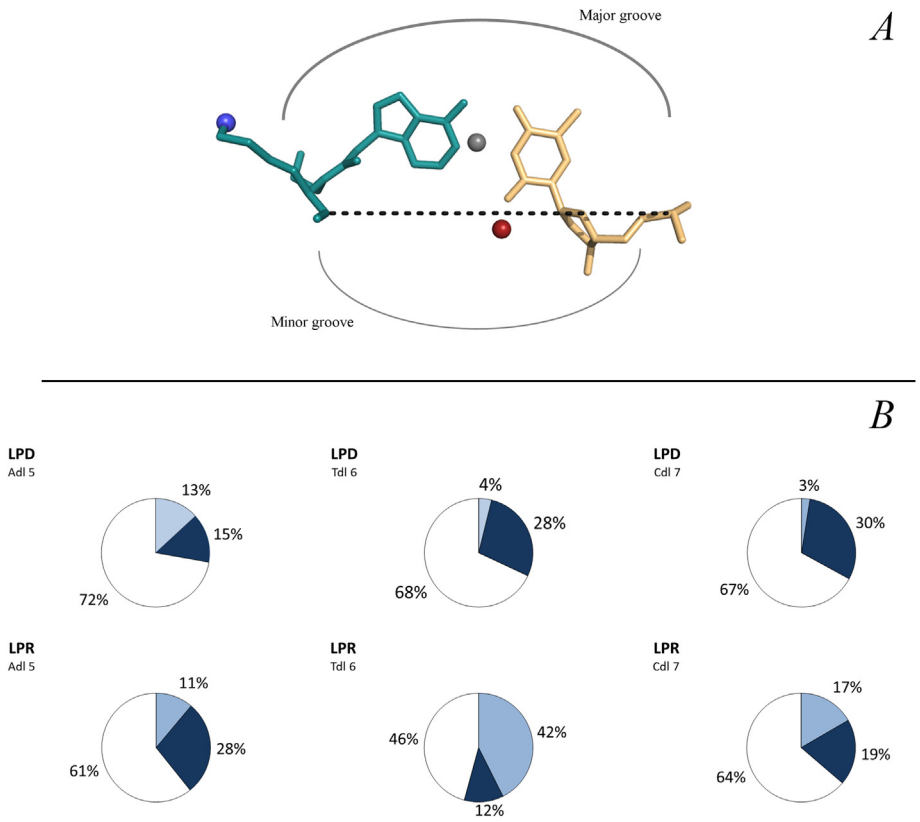

Fig. 5. A: Schematic view of the geometric centers of the Major and Minor grooves (gray and red spheres, respectively) for a generic D-Lys-PNA–DNA couple of interacting residues (Adl5-T6). Nitrogen atom of the lysine side chain is represented as a blue sphere. Two geometric centers were defined for each D-Lys-PNA–DNA pair of interacting residues (Adl5-T6, etc…), to represent the major and the minor grooves, respectively. In details, the center of mass (COM) of the heavy atoms composing the nucleobases moieties represents the geometric center of the major groove region (gray sphere in figure) and the COM computed on the carbonyl oxygen belonging to the PNA backbone and on one of the oxygens of the Phosphate group, represents the center of the minor groove (red sphere in figure). It was assumed that the lysine side chain points towards the major or the minor groove when the position of its nitrogen atom is within a cutoff distance from the geometrical center of these two regions (cutoff 0.8 nm and 0.6 nm for major and minor grooves, respectively). In all the other cases the lysine side chain is considered oriented into the solvent. B: Percentage distributions of the position of the lysine side-chains respect to the major, minor grooves or to the solvent. The position of the lysine side-chains pointing to the major and minor grooves are indicated with light and dark blue, respectively, and those toward the solvent is colored in white. (For interpretation of the references to color in this figure legend, the reader is referred to the web version of this article.)

Please cite this article in press as: I. Autiero, et al., Conformational studies of chiral D-Lys-PNA and achiral PNA system in binding with DNA or RNA through a molecular dynamics approach, European Journal of Medicinal Chemistry (2014), http://dx.doi.org/10.1016/j.ejmech.2014.08.015

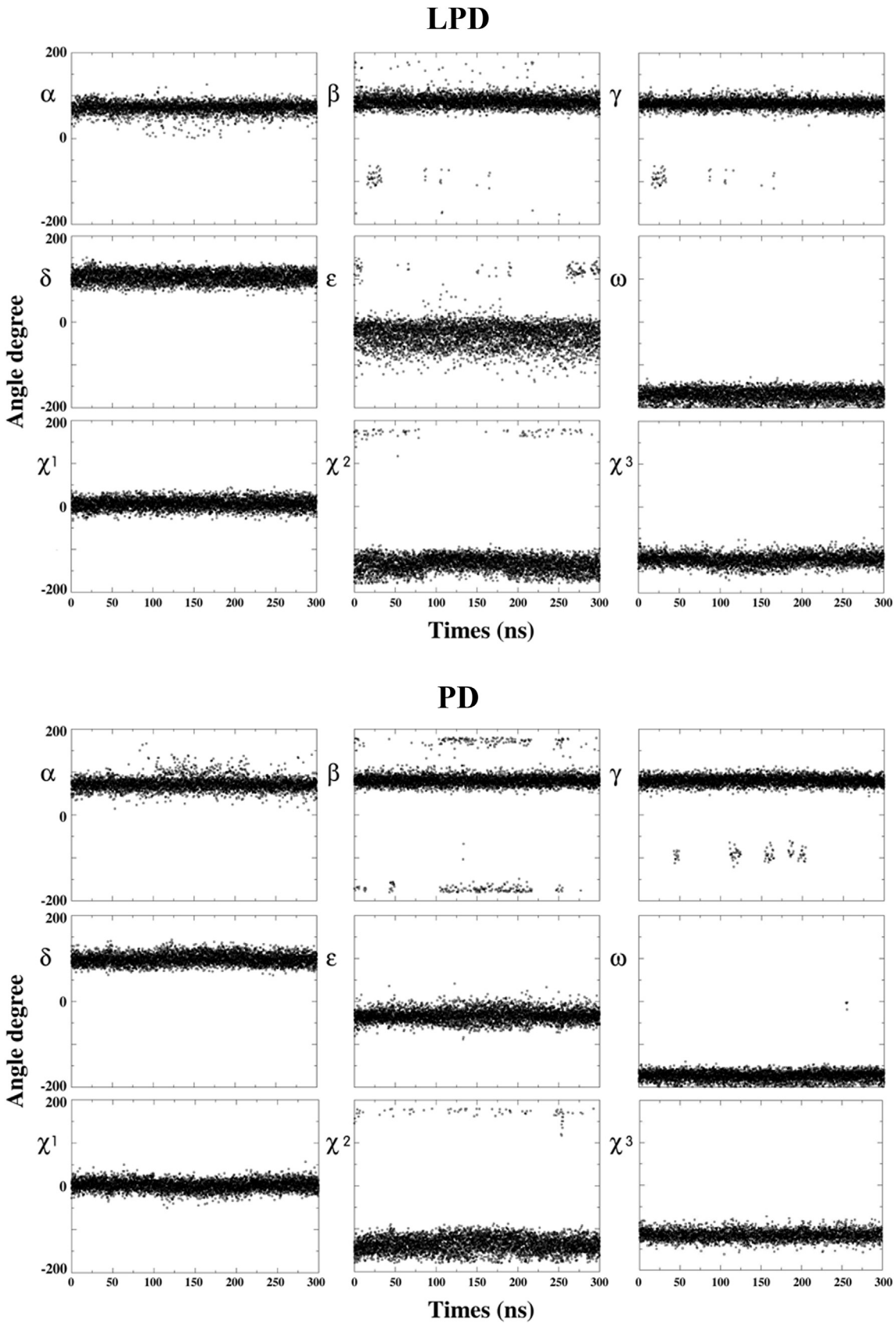

Fig. 6. Variation of the PNA strand torsional angles during each molecular dynamics simulation. Top: LPD. Bottom: PD.

Please cite this article in press as: I. Autiero, et al., Conformational studies of chiral D-Lys-PNA and achiral PNA system in binding with DNA or RNA through a molecular dynamics approach, European Journal of Medicinal Chemistry (2014), http://dx.doi.org/10.1016/j.ejmech.2014.08.015

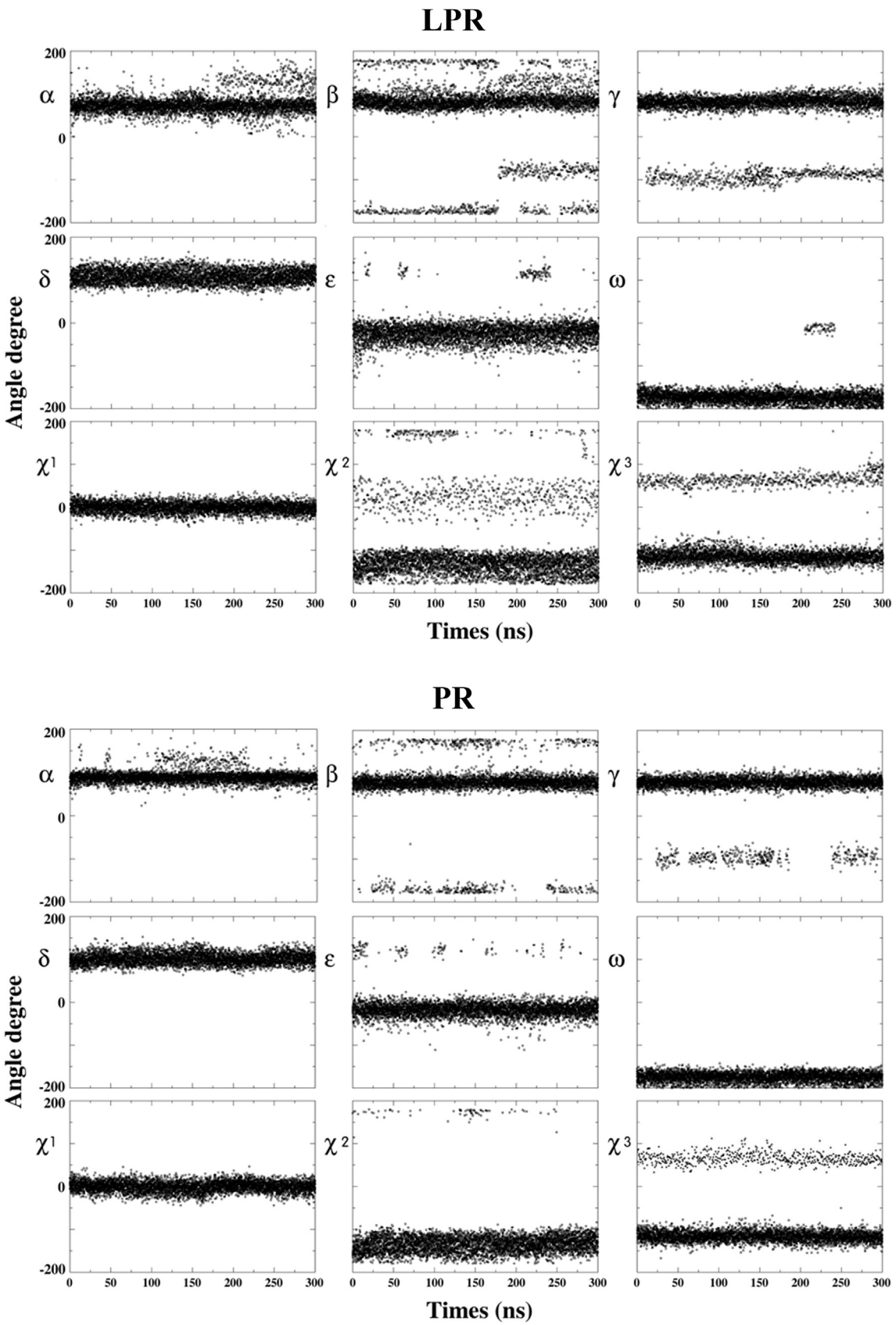

Fig. 7. Variation of the PNA strand torsional angles during each molecular dynamics simulation. Top: LPR. Bottom: PR.

Please cite this article in press as: I. Autiero, et al., Conformational studies of chiral D-Lys-PNA and achiral PNA system in binding with DNA or RNA through a molecular dynamics approach, European Journal of Medicinal Chemistry (2014), http://dx.doi.org/10.1016/j.ejmech.2014.08.015

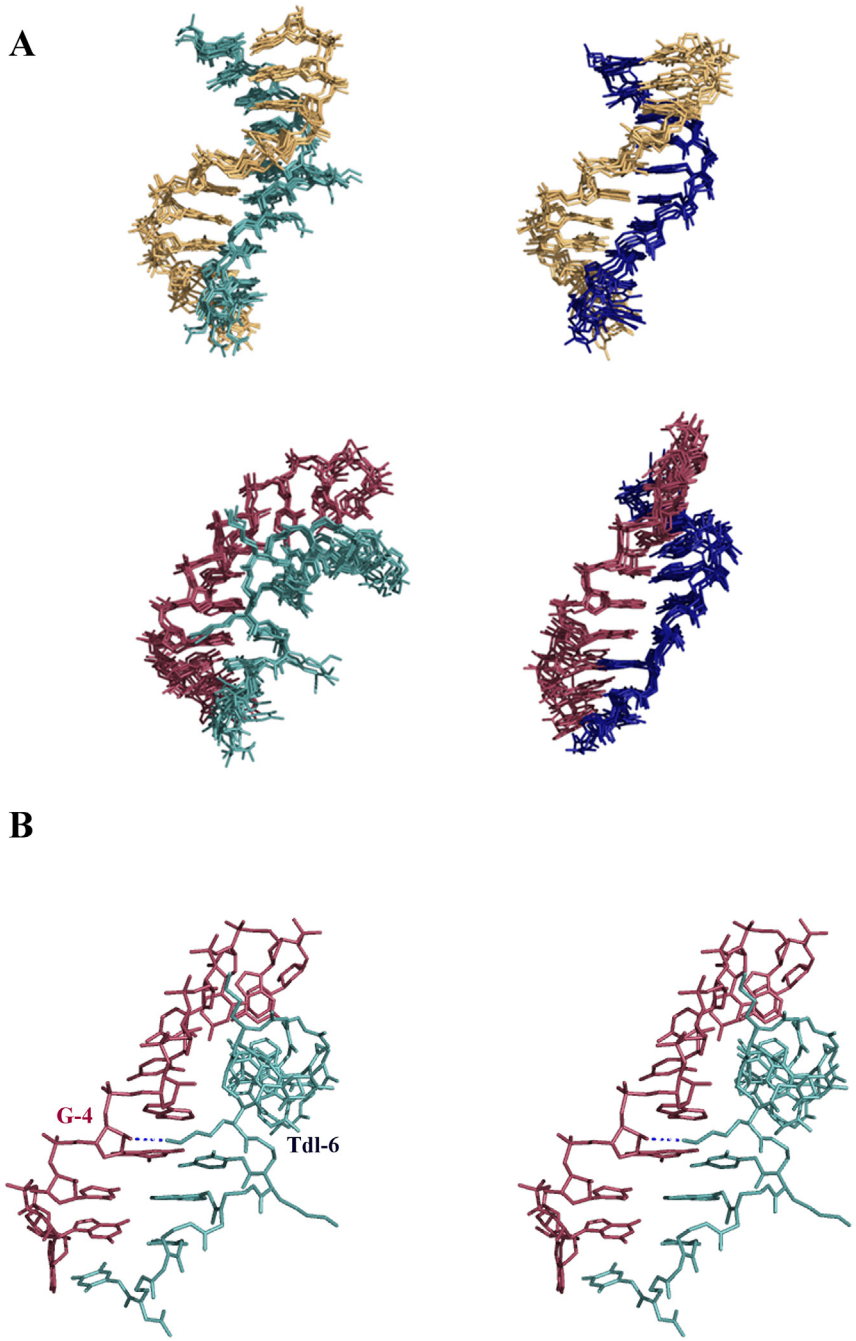

Fig. 8. A. Top: superimposition of 5 MD derived structures of the LPD (left) and PD (right) duplexes. Bottom: superimposition of 5 MD derived structures of the LPR (left) and PR (right) duplexes. B. Stereo-view of a representative structure of the LPR duplex; it is specified the hydrogen bond between the PNA NH_3 moiety in position 6 and the 2′-hydroxyl group of residue 4 of RNA, respectively. The residues are displayed in sticks and colored according to the molecule/oligomer types: DNA in yellow, RNA in red, D-Lys-PNA in cyan and PNA in blue. (For interpretation of the references to color in this figure legend, the reader is referred to the web version of this article.)

corresponding PNA–RNA chiral (LPR) and achiral (PR) heterodimers. All the heterodimers have been subjected to molecular dynamics simulations to provide insight into how the chiral groups, on the PNA backbone, influence the structure and stability of the resulting complexes with either DNA or RNA complementary strands.

LPD and PD systems have been well characterized from previous experimental studies [23,24] showing that D-Lys-PNA binds the complementary DNA exclusively in an antiparallel right handed fashion and has an improved ability to discriminate mismatches in the target complementary DNA with respect to the achiral PNA [23]. Moreover, although the melting temperature of the chiral duplex LPD is slightly lower than that of the corresponding achiral complex, both heterodimers have displayed very similar circular dichroism spectra [49], thus indicating that the presence of the chiral groups marginally lowers stability but does not significantly perturb the conformation of the PNA–DNA antiparallel duplex [49]. Our results are in agreement with these findings, and, indeed, LPD and PD trajectories maintain comparable stability and flexibility during the simulations, with comparable trends in terms of RMSD and RMSF profiles and binding free energy of the complexes, with just a slightly higher stability

Please cite this article in press as: I. Autiero, et al., Conformational studies of chiral D-Lys-PNA and achiral PNA system in binding with DNA or RNA through a molecular dynamics approach, European Journal of Medicinal Chemistry (2014), http://dx.doi.org/10.1016/j.ejmech.2014.08.015

shown by the achiral dimer. In addition, our results indicate a local structural rigidity involving the chiral PNA residues in positions 5, 6 and 7 in the LPD duplex. This structural rigidity is mirrored by the substantially higher percentage of occurrence of WC-hbs in the "chiral box" region of the PNA strand with respect to the corresponding region in the achiral duplex. Interestingly, the capability of D-Lys modified oligonucleotides to locally increase the rigidity of the system has been highlighted also in a previous quantum chemical study on a D-Lys-pTT dimer system [32]. Moreover, our findings are in agreement with the "constrained flexibility" concept previously hypothesized for LPD system by Sforza et al. [24,25,49,50] on intuitive grounds only, and are likely due to the steric hindrance between the lysine side-chains. Indeed, Lys side-chains are bulky, so their conformational freedom is limited/restrained/restricted in order to avoid steric clashes with either PNA backbone atoms or with the other sequentially close Lys side-chains. The local rigidity of the chiral box could explain the improved mismatch recognition ability of D-Lys-PNA that has emerged from experimental studies [23], as previously hypothesized by the X-ray study [23,24], too. In fact, the presence of a mismatch would require a conformational rearrangement of the PNA strand having a high energetic cost due to the structural constraints induced by the presence of D-lysine side-chains.

As to the interaction with an RNA strand, experimental data on our model system are missing; however, previous theoretical studies on systems different from our own have suggested that the PNA–RNA duplex structurally differs from PNA–DNA hybrids [46], and the PNA binding with DNA or RNA has been postulated to be differently affected by the presence of chiral groups on the PNA backbone [50,51], although these structural effects are not yet totally clear. The analysis of our trajectories provides further evidence that WC-hbs represent the main force driving the hybridization between nucleic acid strands. Indeed, the perturbations of the WC-hbs in the central region of the LPR system explains the peculiar behavior of this duplex. These perturbations are likely to be attributable to the electrostatic attraction between lysine charged groups and the phosphates of RNA, or to the propensity of the D-Lys charged group to sporadically enter in contact with the 2′-OH of the RNA (see Fig. 8B). Thus, in the case of LPR, the presence of the charged lysine chains seems to affect in a negative way the stability of the system.

In summary, the results obtained from the comparison between LPD and PD duplexes point out a global similarity and some local differences in their structural preferences, thus providing an explanation for the differences in mismatch recognition abilities of D-Lys PNA monomers, and are able to complement experimental data. On the other hand, our simulations indicate that the hybridization against DNA or RNA is differently affected by the presence of the D-Lys chiral group on the PNA backbone. Indeed, a higher instability is found for the LPR system due to the D-Lys which perturbs the WC-hbs in the central region of the duplex. This instability would be interesting to exploit experimentally and suggests that the addition of three D-Lys groups on the PNA backbone could be used for the development of new PNA-based molecules able to discriminate between DNA and RNA.

Acknowledgments

The authors would like to give their special thanks to Dr Lucrezia Cassano, Dr Caterina Chiarella, Mr Luca De Luca and Mr Giovanni Nasti for technical/administrative assistance. This work was supported by the Fondazione CON IL SUD (2011-PDR-20) and by MIUR-PRIN2009 (20093N774P).

References

[1] P.E. Nielsen, M. Egholm, R.H. Berg, O. Buchardt, Sequence-selective recognition of DNA by strand displacement with a thymine-substituted polyamide, Science 254 (1991) 1497–1500.
[2] M.C. Chakrabarti, F.P. Schwarz, Thermal stability of PNA/DNA and DNA/DNA duplexes by differential scanning calorimetry, Nucleic Acids Res. 27 (1999) 4792–4800.
[3] P.E. Nielsen, M. Egholm, O. Buchardt, Sequence-specific transcription arrest by peptide nucleic acid bound to the DNA template strand, Gene 149 (1994) 139–145.
[4] M. Borgatti, I. Lampronti, A. Romanelli, C. Pedone, M. Saviano, N. Bianchi, C. Mischiati, R. Gambari, Transcription factor decoy molecules based on a peptide nucleic acid (PNA)–DNA chimera mimicking Sp1 binding sites, J. Biol. Chem. 278 (2003) 7500–7509.
[5] B.M. Tyler, K. Jansen, D.J. McCormick, C.L. Douglas, M. Boules, J.A. Stewart, L. Zhao, B. Lacy, B. Cusack, A. Fauq, E. Richelson, Peptide nucleic acids targeted to the neurotensin receptor and administered i.p. cross the blood–brain barrier and specifically reduce gene expression, Proc. Natl. Acad. Sci. U. S. A. 96 (1999) 7053–7058.
[6] M. Komiyama, S. Ye, X. Liang, Y. Yamamoto, T. Tomita, J.M. Zhou, H. Aburatani, PNA for one-base differentiating protection of DNA from nuclease and its use for SNPs detection, J. Am. Chem. Soc. 125 (2003) 3758–3762.
[7] S. Ye, X. Liang, Y. Yamamoto, M. Komiyama, Detection of single nucleotide polymorphisms by the combination of nuclease S1 and PNA, Nucleic Acids Res. Suppl. 2 (2002) 235–236.
[8] F. Pellestor, P. Paulasova, M. Macek, S. Hamamah, The use of peptide nucleic acids for in situ identification of human chromosomes, J. Histochem. Cytochem. 53 (2005) 395–400.
[9] F. Pellestor, P. Paulasova, The peptide nucleic acids (PNAs), powerful tools for molecular genetics and cytogenetics, Eur. J. Hum. Genet. 12 (2004) 694–700.
[10] G. Haaima, H. Rasmussen, G. Schmidt, K.D. Jensen, J.S. Kastrup, P.W. Stafshede, B. Norde, O. Buchardta, P.E. Nielsen, Peptide nucleic acids (PNA) derived from N-(N-methylaminoethyl)glycine. Synthesis, hybridization and structural properties, New. J. Chem. 23 (1999) 833–840.
[11] P. Zhou, M. Wang, L. Du, G.W. Fisher, A. Waggoner, D.H. Ly, Novel binding and efficient cellular uptake of guanidine-based peptide nucleic acids (GPNA), J. Am. Chem. Soc. 125 (2003) 6878–6879.
[12] E. Rozners, Recent advances in chemical modification of peptide nucleic acids, J. Nucleic acids 2012 (2012) 518162.
[13] K.N. Ganesh, V.A. Kumar, Conformationally constrained PNA analogues: structural evolution toward DNA/RNA binding selectivity, Acc. Chem. Res. 38 (2005) 404–412.
[14] K.N. Ganesh, V.A. Kumar, Structure-editing of nucleic acids for selective targeting of RNA, Curr. Top. Med. Chem. 7 (2007) 715–726.
[15] P.E. Nielsen, Peptide nucleic acid. A molecule with two identities, Acc. Chem. Res. 32 (1999) 624–630.
[16] P.E. Nielsen, K.N. Ganesh, Peptide nucleic acids: analogs and derivatives, Curr. Org. Chem. 4 (2000) 931–943.
[17] E. Uhlmann, A. Peyman, G. Breipohl, D.W. Will, PNA: synthetic polyamide nucleic acids with unusual binding properties, Angew. Chem. Int. Ed. Engl. 37 (1998) 2796.
[18] D.A. Braasch, D.R. Corey, Novel antisense and peptide nucleic acid strategies for controlling gene expression, Biochemistry 41 (2002) 4503–4510.
[19] S. Sharma, U.B. Sonavane, R.R. Joshi, Molecular dynamics simulations of cyclohexyl modified peptide nucleic acids (PNA), J. Biomol. Struct. Dyn. 27 (2010) 663–676.
[20] G. Haaima, A. Lohse, O. Buchardt, P.E. Nielsen, Peptide nucleic acids (PNAs) containing thymine monomers derived from chiral amino acids: hybridization and solubility properties of D-lysine PNA, Angew. Chem. Int. Ed. Engl. 35 (1996) 1939–1942.
[21] S. Sforza, G. Haaima, R. Marchelli, P.E. Nielsen, Chiral peptide nucleic acids (PNAs): helix handedness and DNA recognition, Eur. J. Org. Chem. 1 (1999) 197–204.
[22] S. Sforza, T. Tedeschi, A. Calabretta, R. Corradini, C. Camerin, R. Tonelli, A. Pession, R. Marchelli, A peptide nucleic acid embedding a pseudopeptide nuclear localization sequence in the backbone behaves as a peptide mimic, Eur. J. Org. Chem. 1 (2010) 2441–2444.
[23] S. Sforza, R. Corradini, S. Ghirardi, A. Dossena, R. Marchelli, DNA binding of a D-lysine-based chiral PNA: direction control and mismatch recognition, Eur. J. Org. Chem. 2000 (2000) 2905–2913.
[24] V. Menchise, G. De Simone, T. Tedeschi, R. Corradini, S. Sforza, R. Marchelli, D. Capasso, M. Saviano, C. Pedone, Insights into peptide nucleic acid (PNA) structural features: the crystal structure of a D-lysine-based chiral PNA–DNA duplex, PNAS 100 (2003) 12021–12026.
[25] J.I. Yeh, B. Shivachev, S. Rapireddy, M.J. Crawford, R.R. Gil, S. Du, M. Madrid, D.H. Ly, Crystal structure of chiral gamma-PNA with complementary DNA strand: insight into the stability and specificity of recognition an conformational preorganization, J. Am. Chem. Soc. 132 (2010) 10717–10727.
[26] S.C. Brown, S.A. Thomson, J.M. Veal, D.G. Davis, NMR solution structure of a peptide nucleic acid complexed with RNA, Science 265 (1994) 777–780.
[27] M. Eriksson, P.E. Nielsen, Solution structure of a peptide nucleic acid-DNA duplex, Nat. Struct. Biol. 3 (1996) 410–413.

Please cite this article in press as: I. Autiero, et al., Conformational studies of chiral D-Lys-PNA and achiral PNA system in binding with DNA or RNA through a molecular dynamics approach, European Journal of Medicinal Chemistry (2014), http://dx.doi.org/10.1016/j.ejmech.2014.08.015

[28] L. Betts, J.A. Josey, J.M. Veal, S.R. Jordan, A nucleic acid triple helix formed by a peptide nucleic acid-DNA complex, Science 270 (1995) 1838–1841.
[29] E. Wierzbinski, A. de Leon, X. Yin, A. Balaeff, K.L. Davis, S. Rapireddy, R. Venkatramani, S. Keinan, D.H. Ly, M. Madrid, D.N. Beratan, C. Achim, D.H. Waldeck, Effect of backbone flexibility on charge transfer rates in peptide nucleic acid duplexes, J. Am. Chem. Soc. 134 (2012) 9335–9342.
[30] K. Siriwong, P. Chuichay, S. Saen-oon, C. Suparpprom, T. Vilaivan, S. Hannongbua, Insight into why pyrrolidinyl peptide nucleic acid binding to DNA is more stable than the DNA × DNA duplex, Biochem. Biophys. Res. Commun. 372 (2008) 765–771.
[31] J.A. Ortega, J.R. Blas, M. Orozco, A. Grandas, E. Pedroso, J. Robles, Binding affinities of oligonucleotides and PNAs containing phenoxazine and G-clamp cytosine analogues are unusually sequence-dependent, Org. Lett. 9 (2007) 4503–4506.
[32] C.M. Topham, J.C. Smith, Orientation preferences of backbone secondary amide functional groups in peptide nucleic acid complexes: quantum chemical calculations reveal an intrinsic preference of cationic D-amino acid-based chiral PNA analogues for the P-form, Biophys. J. 92 (2007) 769–786.
[33] J. Panecka, C. Mura, J. Trylska, Molecular dynamics of potential rRNA binders: single-stranded nucleic acids and some analogues, J. Phys. Chem. B 115 (2011) 532–546.
[34] P. Weronski, Y. Jiang, S. Rasmussen, Molecular dynamics study of small PNA molecules in lipid-water system, Biophys. J. 92 (2007) 3081–3091.
[35] I. Dilek, M. Madrid, R. Singh, C.P. Urrea, B.A. Armitage, Effect of PNA backbone modifications on cyanine dye binding to PNA–DNA duplexes investigated by optical spectroscopy and molecular dynamics simulations, J. Am. Chem. Soc. 127 (2005) 3339–3345.
[36] R. Soliva, E. Sherer, F.J. Luque, C.A. Laughton, O. Modesto, Molecular dynamics simulations of PNA–DNA and PNA–RNA duplexes in aqueous solution, J. Am. Chem. Soc. 122 (2000) 5997–6008.
[37] S. Sen, L. Nilsson, Molecular dynamics of duplex systems involving PNA: structural and dynamical consequences of the nucleic acid backbone, J. Am. Chem. Soc. 120 (1998) 619–631.
[38] S. Sen, L. Nilsson, MD simulations of homomorphous PNA, DNA, and RNA single strands: characterization and comparison of conformations and dynamics, J. Am. Chem. Soc. 123 (2001) 7414–7422.
[39] I. Autiero, M. Saviano, E. Langella, Molecular dynamics simulations of PNA–PNA and PNA–DNA duplexes by the use of new parameters implemented in the GROMACS package: a conformational and dynamics study, Phys. Chem. Chem. Phys. 16 (2014) 1868–1874.
[40] D. Van der Spoel, E. Lindahl, B. Hess, G. Groenhof, A.E. Mark, H.J.C. Berendsen, GROMACS: fast, flexible, and free, J. Comput. Chem. 26 (2005) 1701–1718.
[41] V. Hornak, R. Abel, A. Okur, B. Strockbine, A. Roitberg, C. Simmerling, Comparison of multiple Amber force fields and development of improved protein backbone parameters, Proteins 65 (2006) 712–725.
[42] A. Perez, I. Marchán, D. Svozil, J. Sponer, T.E. Cheatham, C.A. Laughton, M. Orozco, Refinement of the AMBER force field for nucleic acids: improving the description of α/γ conformers, Biophys. J. 92 (2007) 3817–3829.
[43] H.J.C. Berendsen, J.P.M. Postma, W.F. Van Gunsteren, A. Di Nola, J.R. Haak, Molecular dynamics with coupling to an external bath, J. Chem. Phys. 81 (1984) 3648–3690.
[44] B. Hess, H. Bekker, H.J.C. Berendsen, J.G.E.M. Fraaije, LINCS: a linear constraint solver for molecular simulations, J. Comput. Chem. 18 (1997) 1463–1472.
[45] T. Darden, D. York, L. Pedersen, Particle mesh Ewald-an N.Log(N) method for Ewald sums in large systems, J. Chem. Phys. 98 (1993) 10089–10092.
[46] T. Darden, L. Perera, L. Li, L. Pedersen, New tricks for modelers from the crystallography toolkit: the particle mesh Ewald algorithm and its use in nucleic acid simulations, Structure 7 (1999) R55–R60.
[47] B.R. Miller, T.D. McGee, J.M. Swails, N. Homeyer, H. Gohlke, A.E. Roitberg, MMPBSA.py: an efficient program for end-state free energy calculations, J. Chem. Theory Comput. 8 (2012) 3314–3321.
[48] D.A. Case, T.A. Darden, T.E. Cheatham III, C.L. Simmerling, J. Wang, R.E. Duke, R. Luo, R.C. Walker, W. Zhang, K.M. Merz, B. Roberts, S. Hayik, A. Roitberg, G. Seabra, J. Swails, A.W. Goetz, I. Kolossvai, K.F. Wong, F. Paesani, J. Vanicek, R.M. Wolf, J. Liu, X. Wu, S.R. Brozell, T. Steinbrecher, H. Gohlke, Q. Cai, X. Ye, J. Wang, M.-J. Hsieh, G. Cui, D.R. Roe, D.H. Mathews, M.G. Seetin, R. Salomon-Ferrer, C. Sagui, V. Babin, T. Luchko, S. Gusarov, A. Kovalenko, P.A. Kollman, AMBER 12, University of California, San Francisco, 2012.
[49] T. Tedeschi, S. Sforza, A. Dossena, R. Corradini, R. Marchelli, Lysine-based peptide nucleic acids (PNAs) with strong chiral constraint: control of helix handedness and DNA binding by chirality, Chirality 17 (2005) S196–S204.
[50] A. Calabretta, T. Tullia, R. Corradini, R. Marchelli, S. Sforza, DNA and RNA binding properties of an arginine-based 'Extended Chiral Box' peptide nucleic acid, Tetrahedron Lett. 52 (2011) 300–304.
[51] B. Sahu, V. Chenna, K.L. Lathrop, S.M. Thomas, G. Zon, K.J. Livak, D.H. Ly, Synthesis of conformationally preorganized and cell-permeable guanidine-based gamma-peptide nucleic acids (gammaGPNAs), J. Org. Chem. 74 (2009) 1509–1516.

Please cite this article in press as: I. Autiero, et al., Conformational studies of chiral D-Lys-PNA and achiral PNA system in binding with DNA or RNA through a molecular dynamics approach, European Journal of Medicinal Chemistry (2014), http://dx.doi.org/10.1016/j.ejmech.2014.08.015